SCIENTIFIC REPORTS

OPEN

SUBJECT AREAS:
BIOTECHNOLOGY
BIOPHYSICS

Received
17 February 2014

Accepted
1 August 2014

Published
26 August 2014

Correspondence and requests for materials should be addressed to Y.-Q.Z. (sericult@suda.edu.cn)

Processing and characterisation of a novel electropolymerized silk fibroin hydrogel membrane

Hai-Yan Wang & Yu-Qing Zhang

Silk Biotechnology Laboratory, School of Biology and Basic Medical Sciences, Soochow University; RM702-2303, No. 199, Renai Road, Dushuhu Higher Edu. Town, Suzhou 215123; P. R. China.

Silk fibroin can be made into various forms of biocompatible medical materials, including hydrogel due to its excellent properties. Here, we report a novel method for the preparation of electropolymerized silk fibroin hydrogel membrane (ESFHM), which is formed on a nanoporous film as a barrier using a homemade device at a higher DC voltage. Regenerated silk fibroin solution in Tris buffer (pH 6.55–7.55) was added into a reservoir with a negative charge, and the silk molecules migrated toward the positive charge at 80V_{DC}, resulting in the formation of the ESFHM on the barrier film. Barrier film with a MWCO of 10 kDa is favourable to the formation of the ESFHM. Semi-transparent ESFHM with a swelling ratio of 1056.4% predominantly consisted of a mixture of β-sheets and α-helix crystalline structures. SEM studies revealed that the ESFHM consisted of a 3D mesh structure woven by a chain of silk fibroin nanoparticles with a size of approximately 30 nanometres, similar to a pearl necklace. In vitro studies indicated that the ESFHM was degradable and was sufficient for cell adhesion and growth. Thus, ESFHM is a promising candidate for loading bioactive protein and appropriate cells, as artificial skin or for use in transplantation.

Silk, a well-known natural fibre produced by the silkworm *Bombyx mori* L, consists of fibroin and glue-like sericin. One-third of the fibroin exhibits an amorphous region, and two-thirds of the fibroin demonstrates a crystalline component. The crystalline component consists of two forms, silk I and silk II. Silk II, the structure of the fibre after spinning, mainly consists of an anti-parallel β-sheet that is thermodynamically the most stable[1,2]. Silk I, the conformation of fibroin in the solid state before spinning, is unstable. Many factors can structurally convert silk I into silk II, such as shearing, hydration, heat treatment[3–6], polar solvents and macromolecules that contain carbonyl or polar groups[7–9]. Recently, silk fibroin has been gradually perceived for its biocompatibility, biodegradability, excellent mechanical properties and optical performance. Thus, the development and application of silk fibroin in the field of biomedical materials has gained increasing attention[10–12].

Silk fibroin can be made into various forms of biocompatible materials with different properties and functions using diverse strategies[13,14]. Silk hydrogel, one of the biomaterial forms that has been extensively studied, can be prepared using various methods. Chemical treatments include the addition of glutaraldehyde[15,16] or carbodiimide and other chemicals[17,18] as a crosslinking agent and changing the pH of the environment[19]. Physical methods include vortex, ultraviolet irradiation, and increasing temperature or concentration of silk fibroin[20–23]. Hydrogels synthesised using physical methods generally induce fewer immunogenic reactions during production. Currently, there is a new physical preparation method known as electrogelation, which involves the conversion of liquid silk fibroin into a hydrogel using a lower voltage electric field. Electrogelation is the structural transition of silk fibroin protein in the presence of an electric current. The goal of this study is to design and control the material structure for various biomedical applications[24–26]. Kaplan and colleagues have proposed that when electrodes consisting of pencil lead are immersed in an aqueous solution of silk protein and 25 V_{DC} is applied over 3 min, the solution will begin to gel on the positive electrode. Importantly, this is a reversible process. When the temperature is increased to 60°C or the electrode polarity is reversed, the gel disappears. The obtained gel showed a nice adhesion property, which could be used as a type of reversible and biomimetic adhesive materia[27].

The electrophoretic deposition technique has gained increasing interest due to its short processing time and simple apparatus[28,29]. Zhang et al. used this technique to fabricate a functional coating on titanium implants[30]. Chitosan/silk fibroin composite coatings were deposited onto titanium substrates using this technique at approximately 4°C for 30 s with a voltage of 5 V/cm^{-2}. After electrophoretic deposition, gelatinous coatings accumulated on the surface of the titanium implant, which had a similar macroporous structure with a pore size ranging from

100 to 300 nm. The silk fibroin content in the coatings increased proportionally with the increase of the silk fibroin in the electrophoretic solution, resulting in increased shear and tensile bond strength of the coatings to titanium substrates. In vitro biological tests indicated that the chitosan/silk fibroin composite coatings demonstrated better cellular affinity compared to pure chitosan coatings. Furthermore, the authors proposed that low temperature electrophoretic deposition is an advanced technique for the preparation of functional coatings on titanium surfaces. The same to electrophoretic deposition, Ma et al. fabricated a new material consisting of poly-silk peptides on the surface of a carbon paste electrode and they named this technology electropolymerization. A stable poly-silk peptide film was obtained by scanning 16 cycles in pH 7.4 PBS between −0.5 and +1.5 V[31]. Huang et al. also generated a gel on the positive electrode by applying 25 V_{DC} for 3–5 min using liquid silk fibroin mixed with drug[32]. After freeze-drying, the microspheres of the silk gel were used as a sustained drug release system.

Here, we developed a novel ESFHM using a home-made device. Unlike the technology electropolymerization and other technologies mentioned previously, the ESFHM was formed on the barrier film not the electrodes. Besides, a higher voltage was applied in this experiment. The effect of different conditions on the ESFHM formation was examined, such as electropolymerising buffer, pH, voltage and electropolymerization time. The mechanical and structural properties were carefully studied. In addition, the enzymatic degradation in vitro was also studied, and the biological performance was evaluated using in vitro experiments.

Results

The impact of SDS on the ESFHM formation. We could see that, the hydrogel membrane formed in Tris buffer with SDS was very homogeneous and smooth (Figure 1a). However, the membrane formed in Tris buffer without SDS (Figure 1b) was not homogeneous, and one part of the membrane was milky and the other part was semi-transparent. In addition, the membrane was thin and stiff. These results showed that SDS had a large effect on the ESFHM formation. Furthermore, SDS could cover the surface of the fibroin protein to form a homogeneous globular protein, which made the surface charge of the fibroin protein identical. Thus, the globular protein ran regularly in the buffer. When there was no SDS, the protein concentrated into globular protein with diverse sizes and different surface-charge. During electropolymerization, the protein that was embedded inside had a lower level of denaturation. Thus, the membrane became milky, non-homogeneous and was stiffer than the membrane obtained in buffer with SDS.

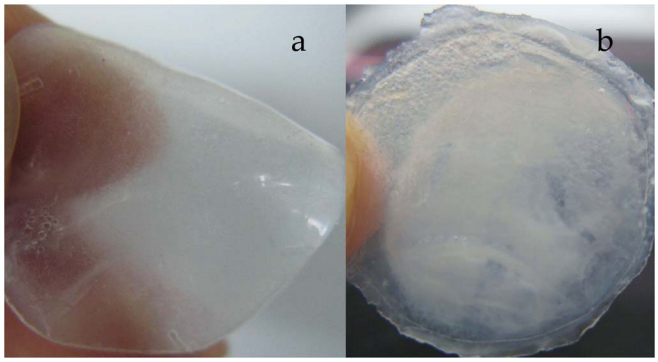

Figure 1 | ESFHMs formed on the barrier film with nanopores in Tris buffer at the voltage of 80VDC. The ESFHMs were formed in pH6.55 Tris buffer with SDS (a) and without SDS (b). In the two photographs, 2 mL of silk aqueous solution (20 mg/mL, UB/LiBr) was added to the cathode chamber.

The morphological features of ESFHM are shown in Figure 2. The ESFHM formed lamellar structures under low magnification (Figure 2a). When the magnification was 50.0 k, the ESFHM formed a network of nanoparticles. A clear border of spherical molecules was found when the magnification was 100.0 k (Figure 2c), and the diameter of the spherical molecule was approximately 30 nm. This result indicated that the silk protein peptide existed in the form of spherical molecules. Silk protein migrated as a globule in the electric field and accumulated as a network structure. Although there was no SDS in the Tris buffer (Figure 2d), the silk proteins still stacked on top of each other in the form of a globule. Only the border of the globule was unclear. These silk fibroin particles were connected with each other in a similar way, except that these particles were stacked more closely.

The influence of different buffer on the corresponding current. To determine the effect of the buffer on the membrane-forming process, three buffers were tested: (1) Tris-HCl buffer – Tris (0.0250 mol/L), glycine (0.192 mol/L) and 0.2% SDS; (2) phosphate buffer – NaH_2PO_3(0.00625 mol/L) SDS (0.2%) and glycine (0.192 mol/L); and (3) Tris-HCl buffer (no SDS) – Tris (0.0250 mol/L) and glycine (0.192 mol/L).

The corresponding current changing trends were similar during the electropolymerization in different buffer systems (Figure 3a). The current (mA) curves were nearly identical between Tris buffers with and without SDS. However, the current in phosphate buffer was much lower than the current in Tris buffer. The corresponding movement of silk fibroin protein was also slower. This result was most likely why the recovery was low when using phosphate buffer as the electropolymerising buffer.

Effect of pH and electropolymerizing time on the recovery of the ESFHM. The recovery of ESFHMs reached the maximum in phosphate buffer at pH 7.55, and the maximum value was reached in the Tris buffer with SDS at pH 6.55 and pH 7.55 (Figure 3b). The recoveries of ESFHMs decreased when the pH decreased or increased. This finding demonstrated that the pH of the buffer had a specific effect on the ESFHM formation. However, the recovery of the hydrogel membrane formed in phosphate buffer was only half the recovery observed in the Tris buffer. This finding showed that phosphate buffer was not conducive to the formation of silk fibroin hydrogel membrane. We proposed that when the same voltage was applied, the resulting electric current changed dramatically among the different buffers. In addition, the velocity of the ions in different groups was vastly different. Thus, the recovery of each group was not likely.

The recovery of ESFHM at the voltage of 80V_{DC} is shown in Figure 3c. The maximal recovery at 97.4% was achieved after 80 min. The value was close to 100%, which indicated that all of the molecules of the regenerated silk fibroin in Tris buffer with SDS migrated to the barrier nano-film and formed a self-assembled hydrogel membrane. After careful observation, there was no membrane but a sticky silk fibroin solution formed within the first 10 min. It was likely that the temperature and pH of the electrophoresis buffer slightly changed in a short period of time. The silk fibroin protein that reached the barrier film did not denature; thus, there was no membrane formed.

The impact of the voltage on the formation of the ESFHM. The voltage had a significant effect on the formation and appearance of the ESFHM (Figure 4). When the voltage magnitude was <50 V_{DC}, there was no membrane formed. When the voltage was too high (100 and 120 V_{DC}), the resulting membrane was stiff and polyporous because it contained many bubbles (Figures 4c and 4d). However, when it was too low (60V_{DC}), the electrolytic rate was very low, and the local temperature and pH of the electropolymerising buffer changed slowly. The resulting membrane was milky and exhibited

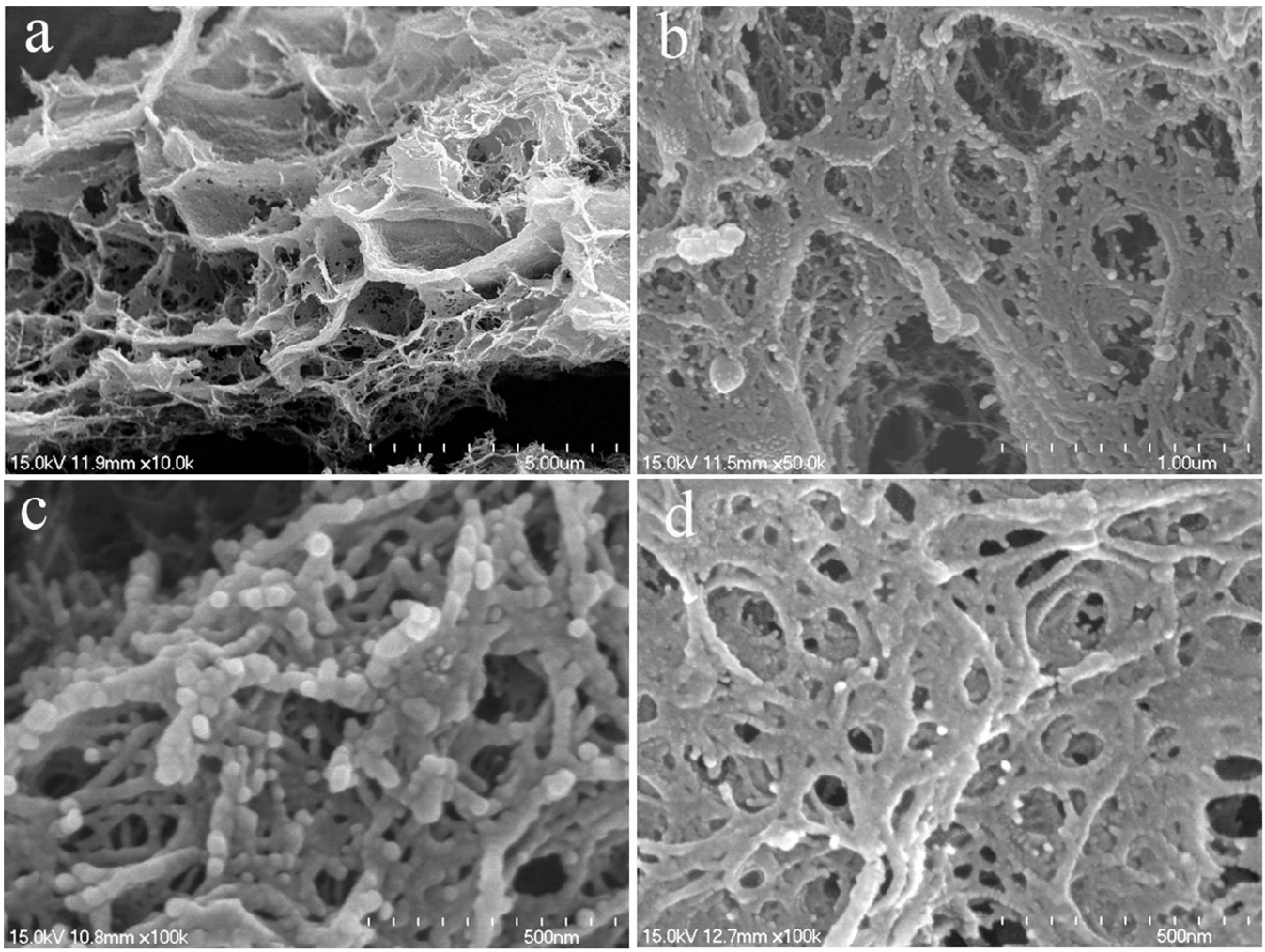

Figure 2 | **SEM photographs of the eSFHM formed in Tris buffer (a,b,c) and Tris buffer (no SDS, (d)) as the same to Figure 2.** (a).×10.0 k; (b) ×50.0 k; (c) ×100.0 k; (d). ×100.0 k.

uneven surfaces (Figure 4a). A homogeneous and smooth hydrogel membrane formed in Tris buffer at 80 V_{DC} (Figure 4b). We speculated that the globular protein slightly denatured during electrophoresis at a low voltage. There was only a thick and slimy protein stuck on the nano-film. However, when a high voltage was applied, the electrolytic rate was fast, and the local temperature rapidly increased. In addition, many bubbles were observed on both of the electrodes, and the protein rapidly denatured. This finding may explain why the membrane was polyporous and stiff.

Effects of regenerated liquid silk fibroin on the recovery and the current. Our study indicated that the silk degumming and fibre dissolution system had effects on the molecular structure and properties of silk fibroin[33]. The breakage degree of the peptide

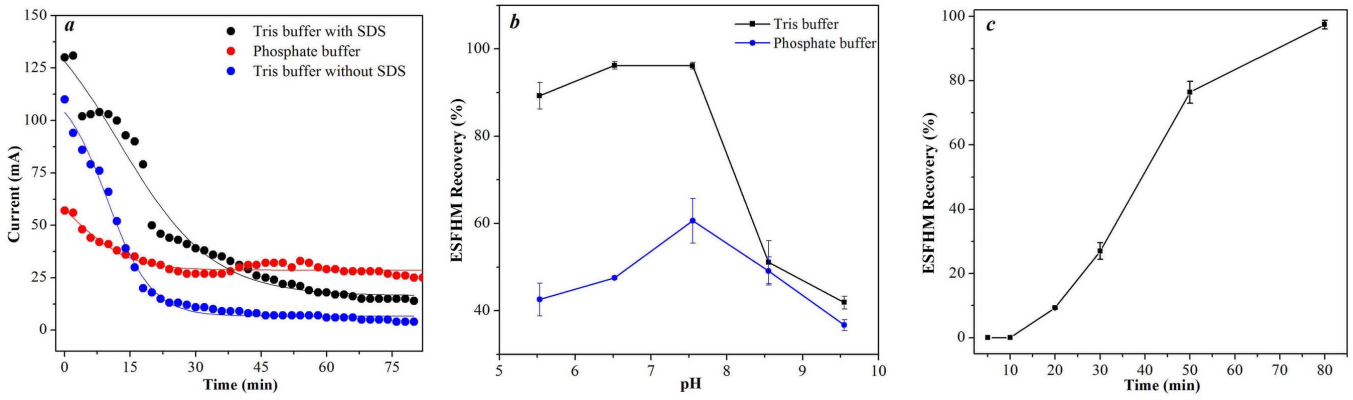

Figure 3 | Variation trend of current in three buffers (a) and recoveries of two buffers with different pH (b) and electrophoresis time (c). (a). the pH of the Tris buffers with and without SDS was 6.55 and the phosphate buffer was 7.55; (b). running for 80 min; (c). runing in Tris buffer (pH 6.55). In all these charts, 2 mL of silk aqueous solution (20 mg/mL, Urea/LiBr) was added to the cathode chamber at the voltage of 80VDC.

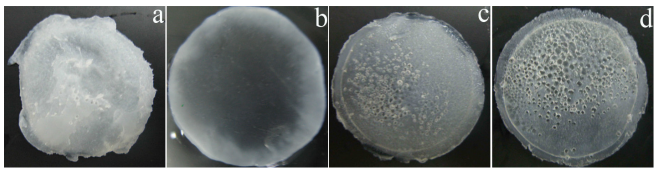

Figure 4 | Images of the ESFHM formed in three voltages of 60VDC (a), 80VDC (b), 100VDC (c) and 120VDC (c). In all the photographs, 2 mL of silk aqueous solution (20 mg/mL, Urea/LiBr, pH 6.55) was added to the cathode chamber and electrolyzing for 80 min.

Table 1 | Effect of the barrier film pore size on the recovery of ESFHM

Barrier-film pore size	ESFHM Recovery (%)
1 kDa	95.3%[a] ± 0.06
10 kDa	99.3% ± 0.11
50 kDa	94.0%[a] ± 0.08

Note: 2 mL of silk aqueous solution (25 mg/mL) was added to the cathode chamber in Tris buffer with SDS (pH 6.55) at the voltage of 80VDC and running for 80 min.
a: 1 kDa, 50 kDa versus 10 kDa ($p < 0.01$).

chain from different liquid silk fibroins was different. To study the effect of the regeneration of liquid silk on the formation and recovery of the ESFHM, six types of liquid silk regeneration methods were studied. These six types of liquid silk in Tris buffer were electropolymerized for 70 min at a voltage of $80V_{DC}$ (Figure 5a). The recovery of the ESFHM was correlated with the breakage degree of the peptide chain. The recovery decreased as the breakage degree increased. The recovery of the UB/LiBr group was significantly higher compared to the SC/TS group and higher then SEAW/TS group. Our preliminary judgment was that the speed velocity of the SC/TS group was slower than the UB/LiBr group at the same time when the same voltage was applied. However, when the electropolymerising time was extended, a higher recovery of the SC/TS group did not occur (data not shown). Thus, we hypothesised that the intact molecules of the regenerated silk fibroin migrated regularly and easily eletrogelated into the ESFHM in the buffer. When the silk peptide was dramatically degraded, the lower molecular weight of the silk peptide was not adopted to form ESFHM. Thus, a low molecular weight of the silk peptide cannot form the ESFHM on the nano-film.

Figure 5b shows the current curves of three types of liquid silk fibroin electropolymerized in Tris buffer at the voltage of $80V_{DC}$. There was little difference among the three samples, which indicated that the current difference resulting from the types of silk fibroin did not have an effect on the recovery of ESFHM.

Effect of the barrier film pore size on the ESFHM formation. The barrier film pore size had an effect on the recovery of the ESFHM to some extent (Table 1). The value was near 100% when the pore size was 10 kDa, which indicated that all of the molecules of regenerated silk fibroin migrated to the barrier nano-film and formed a self-assembled hydrogel membrane. When the pore size was 10 kDa, the recovery of the ESFHM was significantly higher than it of 1 kDa and 50 kDa (Table 1). The pore size of the barrier-film had no effect on the variation trend of the corresponding current, which indicated that the difference in recovery was not due to the corresponding current (Figure 6). These results showed that the barrier film with a MWCO of 10 kDa was the best fit for the formation of the ESFHM.

Effect of regenerated liquid silk fibroin on the swelling properties of the ESFHM. The swelling properties of the three samples had some differences: UB/LiBr > BEW/TS > SC/TS (Table 2). The swelling index of UB/LiBr group was significantly higher than SC/TS group. This finding indicated that the swelling increased as the degradation degree of the silk peptide decreased. The more intact the silk peptide chain, the higher was the recovery of the ESFHM obtained. The greater the order of the membrane structure, the higher was the water-holding capacity of the hydrogel membrane obtained. From an apparent perspective, the membrane formed from the intact silk peptide chain was much softer, which might result in a high water-holding capacity.

The mechanical properties of the ESFHM. *The tensile properties of the ESFHM.* The effect of different preparation methods of regenerated silk fibroin and electropolymerising-buffer systems on the tensile performance of the ESFHM is shown in Table 3. The electropolymerising-buffer system demonstrated an effect. The elongation of the ESFHM formed from Tris buffer was higher than

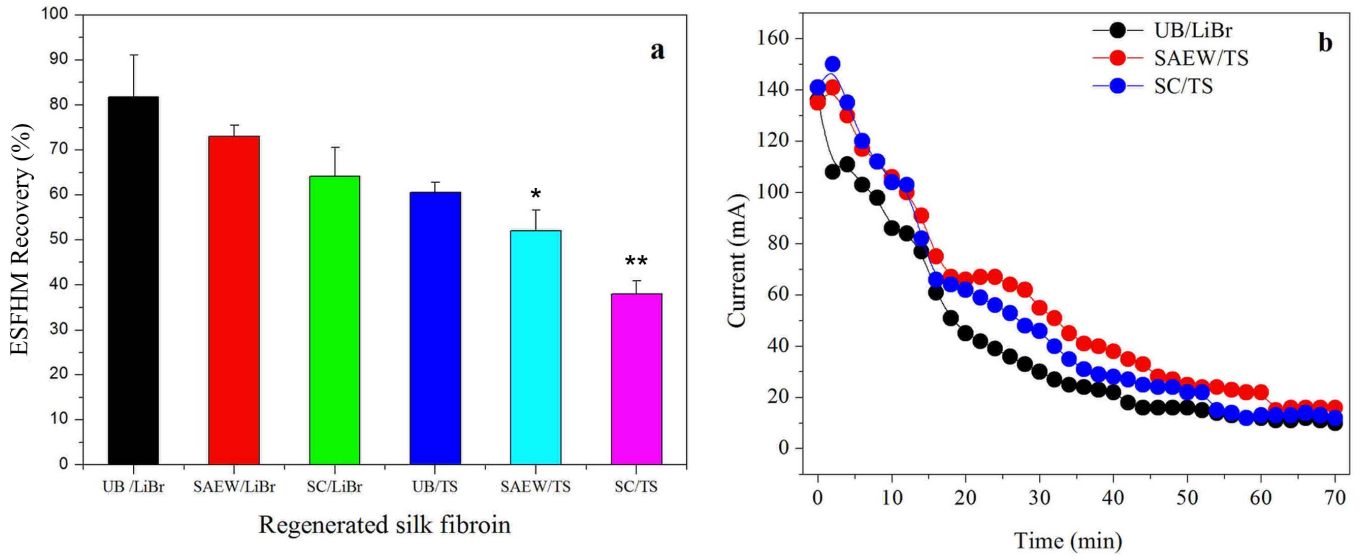

Figure 5 | **Effect of regeneration of liquid silk fibroin on the recovery of ESFHM.** * $p < 0.05$, **$p < 0.01$ (a) and the corresponding current (b) during electrogelation. In the two figures, 2 mL of silk aqueous solution (20 mg/mL) was added to the cathode chamber in Tris buffer with SDS (pH 6.55) at the voltage of 80VDC and running for 70 min.

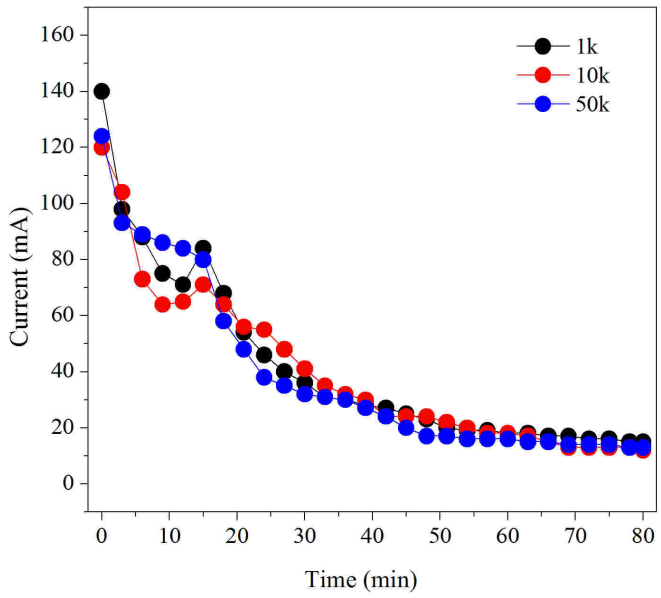

Figure 6 | Variation trend of corresponding current of different-sized barrier film. 1 k: MWCO of 1 kD; 10 k MWCO of 10 kD; 50 k MWCO of 50 kD. 2 mL of silk aqueous solution (25 mg/mL) was added to the cathode chamber in Tris buffer with SDS (pH 6.55) at the voltage of 80VDC and running for 80 min.

that from Tris buffer (without SDS). The silk fibroin protein solution from different preparation methods also had differences when used the same Tris buffer. The breaking force of ESFHM decreased as the degree of degradation increased. In particular, for the SC/TS group, the breaking force was only 27.6% of the UB/LiBr group. These results demonstrated that the electropolymerising-buffer systems had a large effect on the tensile performance of the ESFHM. We obtained membranes with good tensile properties from Tris buffer. The degree of degradation of the silk peptide also had a significant effect, and the more intact the peptide, the better were the tensile properties.

The compression properties of the ESFHM. The LC reflected the softness of the sample. The smaller the LC value, the softer was the sample obtained. The WC embodied the fluffy felling. The sample became fluffier when the value of the WC was larger. The RC reflected the fullness. The samples usually demonstrated good elasticity when there was a large RC value[34]. The test results indicated that the preparation methods of silk fibroin solution had an effect on the compression properties of the ESFHM (Table 4). When the same Tris buffer was used, the intact peptide (UB/LiBr group) elicited better compression properties. In addition, the electropolymerising-buffer systems also had an effect on the ESFHM compression properties. When the same preparation method of silk fibroin solution (UB/LiBr) was used, the compression properties of the ESFHM in Tris buffer (without SDS) were better than in Phosphate buffer. In the following tests, the regenerated silk fibroin solutions were prepared in Tris buffer (pH 6.55) at a voltage of $80V_{DC}$.

The structure properties of the ESFHM. *Spectral characteristics*. Previous studies on the structure of silk fibroin revealed two different structural models: silk I, which is known to be rich in helical structures, and silk II, which is known to be rich in β-sheets[35]. In the literature, amide I (-CO- and -CN- stretching) in the region of 1655–1660 cm^{-1}, amide II (-NH- bending) in the region of 1531–1542 cm^{-1} and amide III (-CN-stretching) in the region of 1230 cm^{-1} were attributed to silk I conformation. However, the infrared absorption peaks of β-sheets in amides I, II and III were observed at 1620–1630, 1515–1530 and 1240 cm^{-1}, respectively, and those of random coils occurred at 1640–1648, 1535–1545 and 1235 cm^{-1}, respectively[36–38]. The membranes had similar spectra for amides II and III with bands at 1523 cm^{-1} and 1231 cm^{-1}, respectively, indicating that the four types of samples were predominantly a mixture of β-sheets and helical structures, as shown in Figure 7. However, there were little differences near amide I. The peaks of the samples treated with methanol shifted from 1654 cm^{-1} to 1631 cm^{-1}, which indicated that the structure of silk I changed into silk II. Our results showed that the secondary structure of the ESFHM was a mixture of β-sheets and helical structures. The β-sheet content of the ESFHM was increased following immersion in methanol. However, its content did not have an evident bearing on air drying.

According to Carey[39], amide I Raman peaks of β-sheets appeared at 1665–1680 cm^{-1} and those of irregular structures at 1660–1670 cm^{-1}. Amide III bands of β-sheets appeared at 1230–1240 cm^{-1} and those of irregular structures at 1240–1260 cm^{-1}. We found that the four samples had similar spectra. However, nuances were observed among the samples, and the film cast from an aqueous solution had spectra in amides I and III with bands at 1666 cm^{-1} and 1254 cm^{-1}, respectively, indicating that the film was a mixture of predominantly random coils and few β-sheets[40–42] (Figure 8). When the film was immersed in methanol, the peaks shifted to 1668 cm^{-1} and 1234 cm^{-1}, which represented β-sheets. After the ESFHM was treated using different methods, the amide I Raman peak was detected at 1666 cm^{-1}, which represented β-sheet structure. The amide III peak was observed at ~1235 cm^{-1}, which was similar to the film immersed in methanol, indicating β-sheets. Air drying of ESFHM and the degradation degree of the silk polypeptide did not have an effect on the Raman spectra of the ESFHM. Thus, the ESFHM predominantly consisted of β-sheets.

X-ray diffraction. Silk fibroin protein mainly occurs in crystalline or amorphous (random coil) form under different conditions. X-ray diffraction (XRD) peaks appear at 12.2°, 19.7°, 24.7° and 28.2° for silk I and at 9.1°, 18.9° and 20.7° for silk II[43,44]. The XRD curves of lyophilized silk fibroin solution (L-SFS) and silk fibroin membrane (SFM) as a control in the experiment had very broad peaks that was a scatter peak at the top, $2\theta = 21.5°$ (Figure 9a). This was a characteristically typical diffraction pattern of amorphous silk fibroin. When the ESFHM was air dried or lyophilised, it existed mainly in crystalline form. After treatment with methanol, lyophilised ESFHM (L-ESFHM) and air dried ESFHM (AD-ESFHM) demonstrated sharper peaks at 20.5° and minor peaks at 24.7°, which represent characteristic peaks of crystalline structure. The results illustrated that L-ESFHM and AD-ESFHM had characteristic diffraction peaks of

Table 2 | Effect of the degradation of peptide on the swelling properties of the ESFHM

	dry mass (mg)		wet mass (mg)		Swelling index (%)	
UB/LiBr	14.10	±0.14	163.00	±10.78	1054.7%	±0.65
BEW/TS	13.80	±0.14	143.60	±7.14	940.3%[a]	±0.41
SC/TS	13.30	±0.28	128.40	±4.17	865.3%[b]	±0.11

a: BEW/TS versus SC/TS ($p < 0.05$);
b: UB/LiBr versus SC/TS ($p < 0.01$).

Table 3 | The tensile properties of the ESFHM

ESFHM No.	Regenerated silk fibroin preparation methods	Buffer systems	Breaking force (cN)	Elongation (%)
1	UB/LiBr	Tris buffer	185.13 ± 27.52	9.86 ± 0.43[a]
2	UB/LiBr	Phosphate buffer	136.13 ± 28.32	11.99 ± 2.17
3	UB/LiBr	Tris buffer (without SDS)	192.63 ± 51.42	5.52 ± 1.74
4	BEW/TS	Tris buffer	64.57 ± 11.24[b]	6.12 ± 1.27
5	SC/TS	Tris buffer	51.04 ± 9.46[b]	4.21 ± 1.82

a: ESFHM No.1 versus ESFHM No.3 ($p < 0.05$);
b: ESFHM No.4, ESFHM No.5 versus ESFHM No.1 ($p < 0.01$).

β-sheet and α-helix crystalline structure. Methanol treatments slightly improved the crystallinity (Figure 9b). Similarly, when SFM was immersed in methanol, the typical diffraction peaks occurred at 20.5° and 24.7°. This showed that the crystallinity of the SFM improved.

DSC thermal property. The DSC curves of the ESFHM for different treatment methods are shown in Figure 10. All of the curves were similar to each other. The thermal decomposition temperatures were between 295 and 297°C. There was no exothermic peak around 200°C, which was attributed to the recrystallisation of silk fibroin and the stable and perfect crystalline formation of the β-sheet conformation induced by the interactions between the fibroin molecular chains on electropolymerization. There was no obvious difference among them, which indicated that lyophilization or air drying had no significant effect on the samples. Although the membranes were immersed in methanol, the thermal decomposition temperature slightly changed. We proposed that most of the ESFHM was β-sheet. Methanol treatment did not dramatically change its structure.

Protease degradation. The enzyme-mediated degradation profiles of the ESFHM were investigated using neutral protease solutions in vitro. The ESFHM was degraded in enzymatic buffer (Figure 11). The degradation rate reached 30% on the first day. In addition, the degradation rate was 71% on the fourth day. The ESFHM in PBS degraded gradually over 4 days, which indicated that there was some protein dissolved in PBS. The enzymatic degradation results showed that the ESFHM was degradable.

Cell metabolic activity on the ESFHM. The MTT assay was performed to quantitatively investigate the cell metabolic activity of L-929 mouse fibroblast cells on the ESFHM after 3, 4 and 5 days in culture. The results obtained from the MTT assay revealed that the number of fibroblasts was increased on the fourth and fifth day (Figure 12B). The cells were able to attach to the ESFHM surface and grew normally (Figure 12A). These results indicated that the ESFHM could satisfy the cell living desires.

Discussion

Kaplan et al. predicted from hydrophobicity plots of the silk protein primary sequence that the protein from reconstituted silk fibroin aqueous solutions existed as micellar structures (100–200-nm diameter)[45]. Our previous results indicated that silk fibroin nanoparticles could be rapidly prepared from liquid silk using water-miscible protonic and polar aprotonic organic solvents. The nanoparticles were insoluble but well dispersed and stable in an aqueous solution and were globular particles with a range of 35 to 125 nm in diameter[46]. There are some studies that have reported that low voltage and SDS could accelerate the denaturation of silk fibroin[25,26,47]. Along these lines, we developed a novel method to form the ESFHM. SDS from the electropolymerizing buffer could combine with the positive charge groups of the surface of the fibroin protein to form homogeneous globular protein with a negative surface charge similar to protein electrophoresis. During electrophoresis, the protein globules migrate regularly from the cathode to the anode. Due to the proton motive, local pH changes and the obvious temperature increase during electrophoresis, the silk fibroin protein denatured gradually and was intercepted by the barrier nano-film, and the silk fibroin micelles were then orderly stacked similar to a pearl necklace and finally formed the ESFHM. The movements of the proton and small molecules with a charge, such as Tris buffer, were not affected by the barrier nano-membrane, and these were still able to pass freely through the membrane (Figure 13).

The nanoporous film as a barrier between the two electrodes used in this experiment differed from previous methods. The ESFHM was formed on the barrier other than the surface of the electrodes[27]. The ESFHM was soft, smooth and had a fixed form and showed a high swelling ratio of up to 1056.4%.

Kojic et al. developed a finite-element model that described how ion electrodiffusion controls E-gel growth[26]. The calculated rectangular pH profile was consistent with the experimentally measured profile, indicating that ion electrodiffusion governs pH distribution and is thus central to electrogelation. In addition, other studies found that the silk electrogelation was based on local pH changes as a result of water electrophoresis. Silk fibroin has a pI = 4.2 and E-gel forms when <pI. However, we found that the pH changed during electropolymerization, with a final pH > 8 in the cathode chamber and pH < 4 in the anode chamber. The formation of ESFHM occurs in an alkaline environment. To better understand this problem, we performed further tests. The positions of the anode and cathode were adjusted to have the same distance to the nano-film. After electro-

Table 4 | The compression properties of the ESFHM

ESFHM No.	RSF Prep. method	Electropolymerizing-buffer systems	LC (Compression Linearity/softness)		WC(gf/cm²) (Compression ratio var/fluffy)		RC(%) (Compression elasticity/fullness)	
1	UB/LiBr	Tris buffer	0.30	±0.051	0.40	±0.030	15.45	±7.986
2	UB/LiBr	Phosphate buffer	0.24	±0.032	0.27	±0.136	10.35[c]	±2.839
3	UB/LiBr	Tris buffer (without SDS)	0.20	±0.075	0.29	±0.100	25.12	±3.498
4	BEW/TS	Tris buffer	0.41	±0.075	0.20[a]	±0.117	8.76	±3.961
5	SC/TS	Tris buffer	0.43[a]	±0.055	0.24[b]	±0.092	6.28[a]	±4.345

a: ESFHM No.4, No.5 versus ESFHM No.1 ($p < 0.05$);
b: ESFHM No.5 versus ESFHM No.1 ($p < 0.01$);
c: ESFHM No.2 versus ESFHM No.3 ($p < 0.01$).

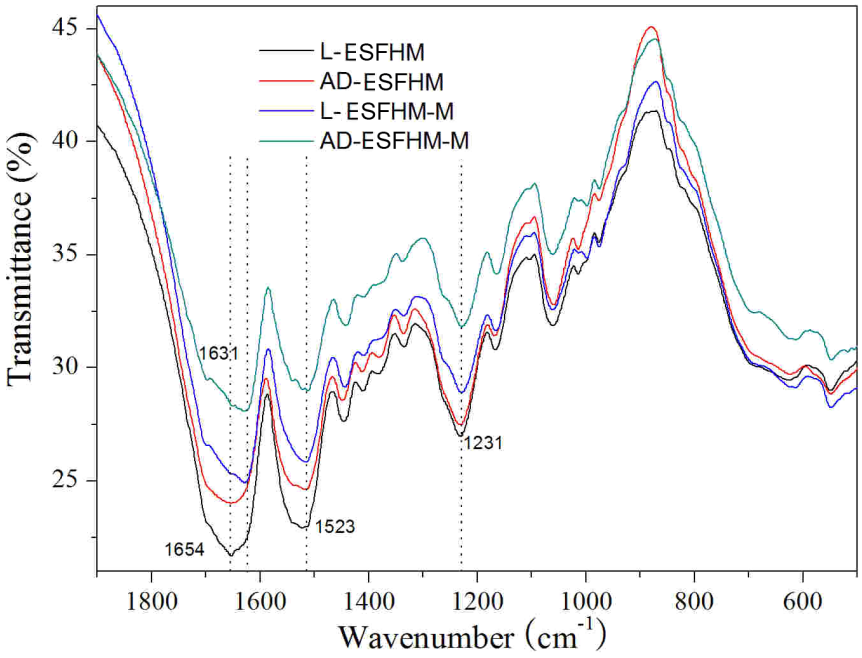

Figure 7 | FT-IR spectra of the various ESFHM. Silk aqueous solution was regenerated by UB/LiBr method. L-ESFHM: ESFHM was frozen at −20°C and lyophilised; AD-ESFHM: ESFHM was air dried in the fuming cupboard; L-ESFHM-M: L-ESFHM was soaked in 80% (v/v) methanol for 20 min; AD-ESFHM-M: AD-ESFHM was soaked in 80% (v/v) methanol for 20 min.

polymerization, we also successfully obtained the ESFHM. These results indicated that the formation of a hydrogel membrane might not be completely induced by local acidic pH. Lu et al. inferred that the repulsive forces from the negative surface charge of the acidic groups on the protein were screened by the local decrease in solution pH in the vicinity of the positive electrode[25]. These results emphasised the importance of the H^+. To confirm whether this theory applied to our experiment, we made a small change in our setup. The distance between the negative electrode and barrier nano-film was decreased to 1 cm. After the electrophoresis process, we obtained the ESFHM from the nano-membrane. However, the recovery of the ESFHM was lower and we found some gel-like protein suspended in the cathode chamber. This phenomenon may be caused by the bubbles originating from the cathode. The protein microballoons originally migrated to the nano-film and were blown over by the bubble. These results indicated that the formation of the

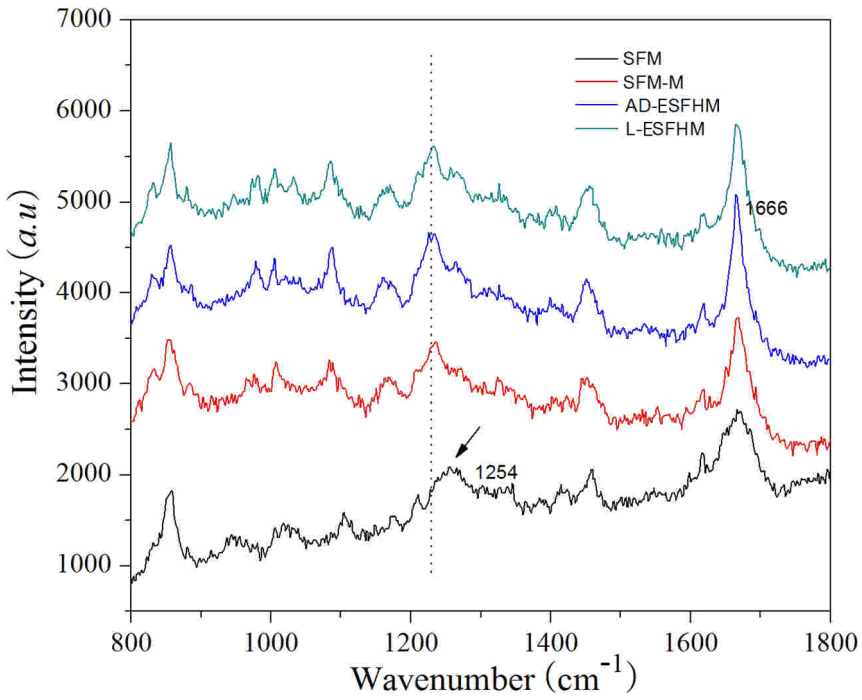

Figure 8 | Raman spectra of the various ESFHM before and after methanol immersion. SFM: the silk fibroin solution was dropped onto a PVC plate using a pipette and then air-dried at 25°C; SFM-M SFM was soaked in 80% (v/v) methanol for 30 s; L-ESFHM: ESFHM was frozen at −20°C and lyophilised; AD-ESFHM: ESFHM was air dried in the fuming cupboard.

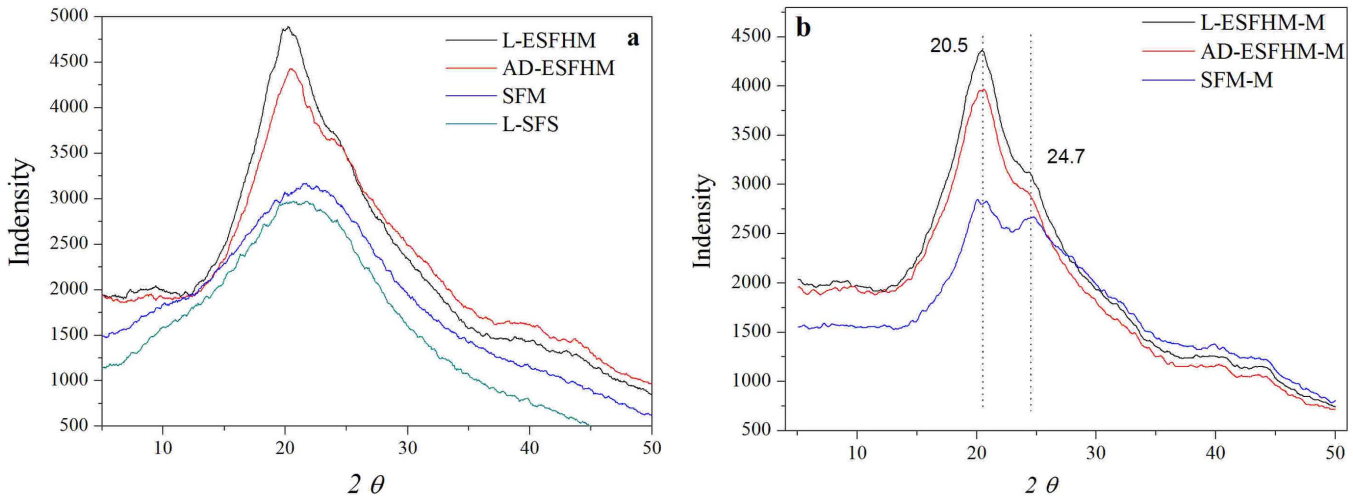

Figure 9 | X-ray diffraction curves of ESFHMs and treated ESFHMs. (a) X-ray diffraction curves of lyophilized silk fibroin solution (L-SFS), SFM and AD-ESFHM (formed in Tris buffer, pH 6.55, by UB/LiBr). (b) X-ray diffraction curves of SFM, lyophilized and AD-ESFHMs after methanol immersion.

membrane is not completely induced by local H^+. To examine whether the temperature has an effect on the recovery of the ESFHM, we put the setup in an external ice bath. Interestingly, we only obtained a thin slice of ESFHM, which demonstrated that temperature played an important role in the ESFHM formation process. The protein cannot denature when the temperature is too low.

The ESFHM-forming mechanism involves the transition of an aqueous silk fibroin solution to a hydrogel membrane state in the presence of an electric current and SDS in Tris buffer. The electric field, as the driving force of silk protein movement and the fuse of the ESFHM formation, can change the temperature and pH of the electrophoresis buffer. The local environmental change, in particular temperature change, and the combination with SDS may result in the denaturation of silk fibroin protein. However, details of the potential electric field-induced structural changes were not detectable using the current experimental techniques.

The ESFHM is a type of novel material with excellent appearance and good mechanical features. It is a promising candidate for loading bioactive protein and appropriate cells or using in transplantation. Future work will focus on the ongoing experiments in cell culture and mice to provide a foundation for the use of this novel biomaterial.

A type of soft ESFHM with a smooth surface was successfully prepared on the barrier nano-film in the DC electric field with a higher voltage. Similar to protein electrophoresis, SDS from the electropolymerising buffer played a key role in the formation of the ESFHM, particularly its semi-transparent and membrane uniformity. The high recovery of the ESFHM with moderate mechanical properties was formed on the barrier film with a moderated nanoporous size in Tris buffer (pH from 6.55 to 7.55) at $80V_{DC}$. Not only did the buffer contain SDS, but the regeneration methods of liquid silk fibroin also had an effect on the formation of the ESFHM. The analytical results of the structure showed that the ESFHM was predominantly a mixture of β-sheets and α-helix crystalline structures. To a lesser degree, methanol treatment improved the crystallinity of the ESFHM. The preliminary in vitro biological tests indicated that the ESFHM was a 3D scaffold, which was degradable and was sufficient for cell adhesion and growth requirements. The novel hydrogel membrane with moderated mechanical properties and biodegradable and biological compatibility is a promising candidate

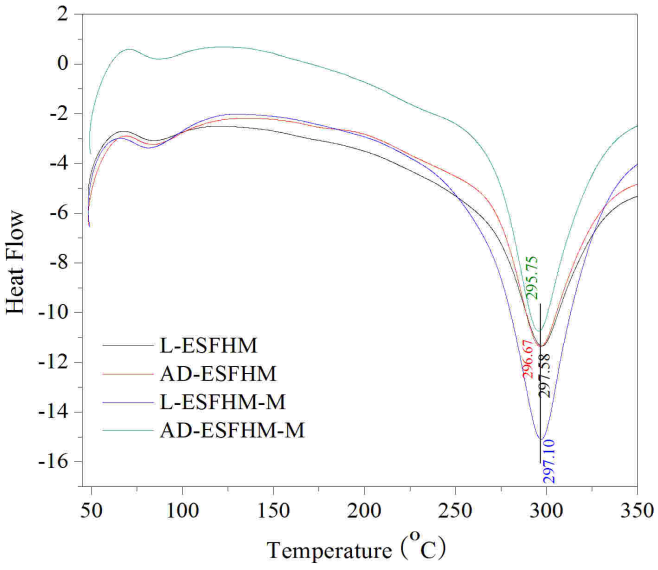

Figure 10 | Thermal properties of the ESFHMs before and after methanol immersion. The ESFHM was formed in Tris buffer (pH 6.55) by UB/LiBr method.

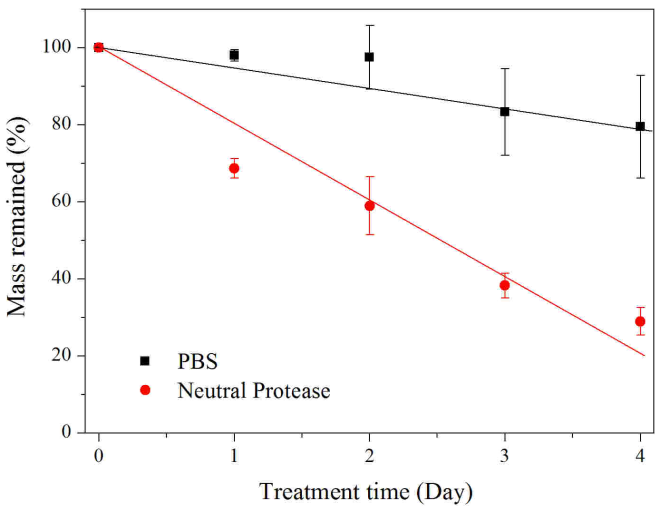

Figure 11 | Mass remained of the ESFHM (formed in Tris buffer, pH 6.55 by UB/LiBr method) during enzymatic degradation.

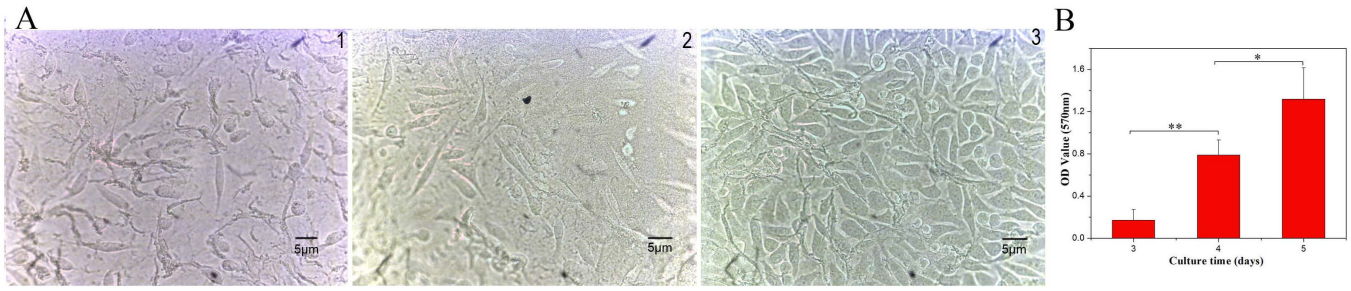

Figure 12 | Images of L-929 mouse fibroblasts cells on the ESFHM (formed in Tris buffer, pH 6.55 by Urea/LiBr) surface for days 3, 4 and 5(A). MTT analysis of the L-929 mouse fibroblasts cells after 3, 4 and 5 days seeded on the ESFHMs.* $p < 0.05$, **$p < 0.01$(B).

for loading bioactive protein and appropriate cells or for use in transplantation.

Methods

Preparation of regenerated silk solution. Silk fibroin solution was prepared from silkworm cocoons according to procedures described in our previous study[33]. Three silk degumming and two fibroin fibre dissolution methods were tested. Degumming by urea buffer (UB) was performed by heating in 8 M aqueous urea containing 0.04 M Tris-SO_4 (pH 7.0) and 0.5 M mercaptoethanol for 2 h at 80°C[48]. The shell was degummed twice in boiling 0.2% (w/v) Na_2CO_3 solution (SC) for 0.5 h[49]. The strong alkaline electrolysed water degumming method (SAEW) was performed 25 times (v/w) in SAEW (pH 11.50) for 30 min at 100°C[50]. After these degumming treatments, the resulting silk materials were washed repeatedly in deionised water and then air-dried. The degummed silk fibres were added to 20 times (v/w) 9.3 M LiBr (LiBr) and Ajisawa's reagent ($CaCl_2$/ethanol/water, 1 : 2 : 8 molar ratio, short TS).

After the silk fibroin/salt solution was filtered through deionised water or centrifuged at 8000 rpm for 10 min, the filtered solution or supernatant was continuously dialysed for 48 h against running water to remove $CaCl_2$, smaller molecules and some impurities using a cellulose semi-permeable membrane (cut-off 5 kDa). Six aqueous solutions of silk fibroin were used for the preparation of ESFHM.

Experimental setup. The experimental setup consisted of two electrodes made of platinum wire. The negative electrode (cathode) in the inner chamber and the positive electrode (anode) in the outer chamber were separated by a nano-membrane and its support (Figure 14). Prior to electropolymerization, 20 mL of electropolymerising buffer and 2 mL of silk fibroin aqueous solution (20 mg/mL) were mixed and added into the inner chamber, and 30 mL of the same buffer was added to the outer chamber. The electrodes were electrically connected using alligator clips to the top of the platinum wire to a programmable direct-current (DC) power supply. The closed electrical circuit consisted of the following: power supply → (+) electrode → silk solution → (−) electrode → power supply. When these groups of positive electric charge on the surface of silk fibroin molecules were combined with SDS with a negative electric charge, the silk fibroin molecules migrated toward the anode in electropolymerization buffer. After running for 30–40 min, the semi-transparent hydrogel membrane was formed on the barrier film with nanopores (nano film).

Post-processing methods of ESFHM. Three post-processing methods were adopted to improve the properties of the ESFHM. ①ESFHM was soaked in 80% (v/v) methanol for 20 min and then drained on paper towels (ESFHM-M). ②ESFHM was air dried in the fuming cupboard (AD-ESFHM). ③ESFHM was frozen at −20°C and lyophilised (L-ESFHM). As a control, the silk fibroin solution was dropped onto a PVC plate using a pipette and then air-dried at 25°C (SFM). SFM was soaked in 80% (v/v) methanol for 30 s and then drained using paper towels (SFM-M).

Swelling ratio measurement. To evaluate the ESFHM swelling, the samples were immersed in deionised water for 24 h at 37°C. After the excess surface deionised water was removed with filter paper, the swollen weight of each membrane was recorded. The samples were then dried in the fume hood to obtain the dry weight. The swelling ratio for each sample was calculated using the following equation: % swelling = (Ws − Wd)/Wd × 100, where Wd is the dry weight of the construct and Ws is the swollen weight of the construct[51]. The samples were measured repeatedly three times per group.

Mechanical property test. The mechanical properties of the gel samples were tested in the wet state in PBS at room temperature. The tensile properties of the ESFHM were measured using a testing machine (INSTRON model 3365; Universal Testing Machine, INSTRON, US). The length between the grip anchors was 0.5 cm. The tests were performed at a strain rate of 10 mm/min. Sample deformation and strain combined with the stress–strain curves were obtained using software analysis. The compression performance was analysed using the KES-FB3-type Compression Tester (KATO TECH CO, LTD).

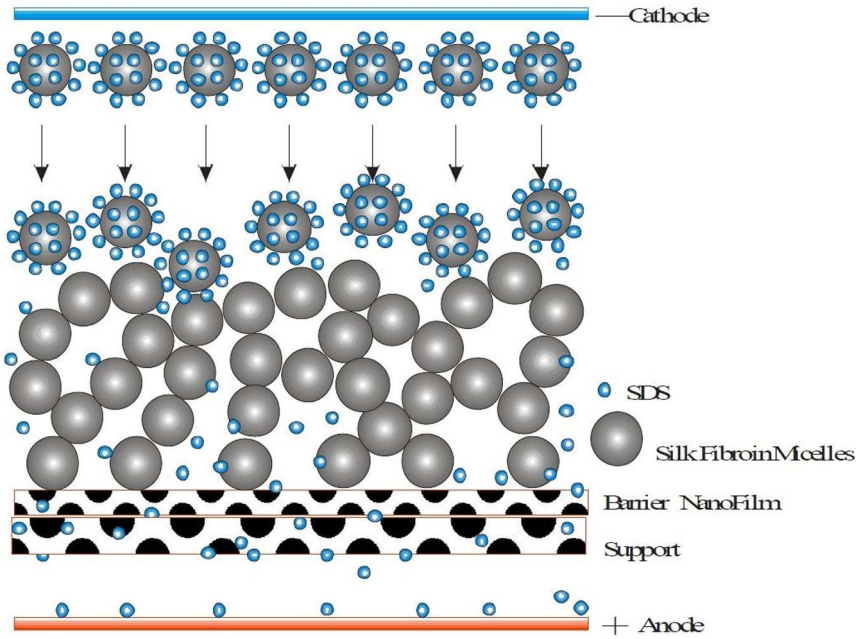

Figure 13 | The schematic diagram of the ESFHM formation.

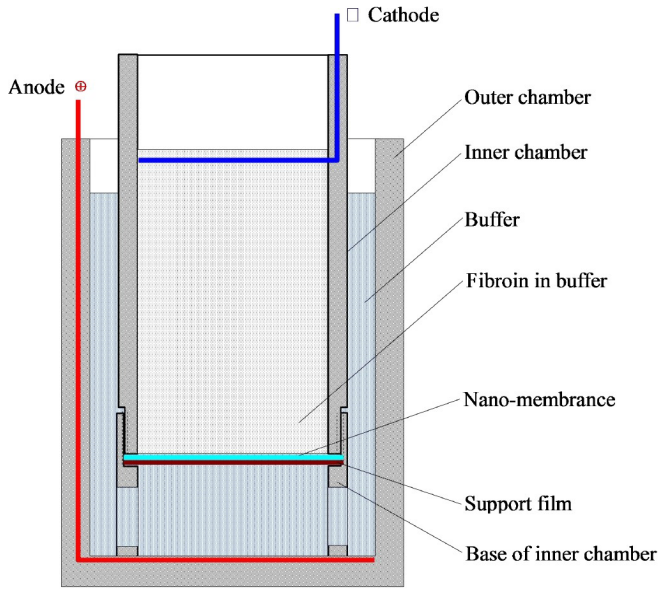

Figure 14 | Schematic diagram of the ESFHM formation.

Structure analysis. The IR Spectra of ESFHM was obtained using an FTIR spectrometer (Nicolet 6700; Thermo Fisher, USA) in the spectral region of 4000 − 400 cm^{-1} to determine the molecular conformation. For each measurement, scanning was repeated 16 times with a resolution of 4 cm^{-1}. Ten-point smoothing was used for the IR spectroscopy. A Microscopic Confocal Raman Spectrometer (LabRAM HR800, Horiba JobinYvon), which was equipped with a LMPLFL optical microscope (50× objective with an aperture of 400 μm) was used to analyse the surface texture of the ESFHM at a wavelength range of 400–4000 cm^{-1} at a resolution of 4 cm^{-1}. The wavelength of the laser was 633 nm, and the samples were irradiated for 20 s during spectrum recording. Adjacent averaging ten-point smoothing was used for Raman spectroscopy. Thermal analysis of the ESFHM was performed using a differential scanning calorimeter (DSC) instrument (DSC 2010, TA Instruments) at a heating rate of 20°C/min in the temperature range of 50 to 350°C. X-ray diffraction analysis of the ESFHM was performed using an X-ray diffractometer (X'Pert-Pro MPD, PANalytical) recording spectra in the angle range of 5 to 50 degrees (2θ).

SEM observation. To characterise the internal microstructures of the ESFHM, the hydrogel membranes were dually fixed using a glutaraldehyde-osmium tetroxide fixative. After rinsing with PBS, the samples were cut to expose the cross-sections and coated with Pt/Pd using a sputter coater (SP-2 AJA Sputtering System). The samples were observed using a scanning electron microscope (Hitachi S-4700, Japan) under an accelerating voltage of 15 kV. At least five images from the samples for each group were used for quantification.

Enzymatic degradation in vitro. To characterise the enzymatic degradation properties of the ESFHM, the hydrogel membrane samples were dried in a fume hood and the ratio of wetting-drying was calculated. Next, the wet samples were placed in Erlenmeyer flasks with 0.05 M phosphate buffer (PBS), pH 8.0, containing 1 U/mL neutral protease at 37°C (bath ratio 1 : 50, wet W/V). At a predefined time, the samples for each condition were removed. The mass loss was determined by the ratio of final weight to the original dry weight. The sample size was three membranes per group.

Cell culture. L-929 mouse fibroblasts cells were obtained from the Institute of Cell Biology, Chinese Academy of Sciences (Shanghai, P.R. China). The cells were maintained in Dulbecco's Modified Eagle's Medium (DMEM) with DMEM-H30243.01B (Thermo HyClone) with 10% bovine serum albumin and 1% penicillin/L-glutamine and cultured in a standard cell culture incubator (HERAcell 240i) in a 5% CO_2 atmosphere at 37°C. The cell culture medium was changed every 2 days. The cells were passaged twice a week when confluence was achieved.

Cell morphology and cell metabolic activity measurement. The cell metabolic activity on the surface of the ESFHM was measured using an MTT colorimetric assay. The membranes were cut to diameters of 1 cm and immersed in 75% (v/v) ethanol for 48 h and thoroughly rinsed with sterilised DPBS. The sterilised membranes were then added to each well of a 48-well plate and preconditioned with cell culture medium overnight prior to cell plating. Next, 100 μL of L-929 mouse fibroblast cell suspension was seeded onto the membrane surface at a density of 1.5×10^4 cells $well^{-1}$. Three wells were set for each group. The culture medium was changed every day. At a predetermined time, the plates were removed and visualised using fluorescence microscopy (Nikon Eclipse TE 2000-U, Japan). After observation, 500 μL of 5 mg/ml 3-(4, 5-dimethylthiazol-2-yl) -2,5-diphenyl tetrazolium bromide (MTT) solution was added to each well. After a 4-h incubation, the supernatant was carefully removed and 500 μL of dimethyl sulfoxide solution was added to dissolve the formazan crystals. After agitation for 10 min, the absorbance was read at 570 nm using a microplate reader (SpectrMax M5, Molecular Devices, Sunrise, USA). Three replicates were averaged for each membrane sample.

Statistical analysis. Samples for all quantifiable analyses were n = 4–5 with each biological replicate having technical duplicates. The ESFHM and cell morphology analysis were performed at n = 3, only representative images are shown. Unless otherwise noted, data were expressed as mean ± standard deviation (SD) and were analyzed using one-way ANOVA with a post hoc t-test, adopting a 5% ($P < 0.05$) level of significance.

1. Lotz, B. & Cesari,C. F. The chemical structure and the crystalline structures of *Bombyx mori* silk fibroin. *Biochimie.* **61**, 205 (1979).
2. Wen, D. J., Wang, H., Zhu, X. S. & Sun, J. P. Conformation and crystallinity of silk fibroin. *J. Textile. Res.* **26**, 110–112 (2005).
3. Magoshi, J. & Magoshi, Y. Physical properties and structure of silk V: Thermal behavior of silk fibrion in the random-coil conformation. *J. Polym. Sci B-Polym. Phys.* **15**, 1675–1683 (1977).
4. Ishida, M., Asakura, T. & Yokoi, M. Solvent and mechanical-treatment-induced conformational transition of silk fibroin studied by high-resolutionsolid-state ^{13}C NMR spectroscopy. *Macromolecules.* **23**, 88–94 (1990).
5. Tsukada, M., Nagura, M. & Ihikawa, H. Structural changes in poly(L-alanine)inducedby heat treatment. *J. Polym. Sci B-Polym. Phys.* **25**, 1325–1329 (1987).
6. Magoshi, J., Mizuide, M. & Magoshi, Y. Physical properties and structure of silkVI: conformational changes in silk fibroin induced by immersionin water at 20°Cto 130°C. *J. Polym. Sci B-Polym. Phys.* **17**, 515–520 (1979).
7. Tsukada, M., Freddi, G., Monti, P., Bertoluzza, A. & Kasai, N. Structure and molecular conformation of tussah silk flims: effect of metharnol. *J. Polym. Sci B-Polym. Phys.* **33**, 1995–2001 (1995).
8. Lee, K. Y. & Ha, W. S. DSC studies on bound water in silk fibroin/s-carboxymethyl kerateine blend films. *Polymers.* **40**, 413l–4134 (1999).
9. Park, S. J., Lee, K. Y. & Ha, W. S. Structural changes and their effect on mechanical properties of silk fibroin/chitosan blends. *J. Appl. Polym. Sci.* **74**, 257l–2575 (1999).
10. Veparia, C. & Kaplan, D. L. Silk as a biomaterial. *Prog. Polym. Sci.* **32**, 991–1007 (2007).
11. Gil, E. S., Panilaitis, B., Bellas, E. & Kaplan, D. L. Functionalized Silk Biomaterials for Wound Healing. *Adv. Healthcare. Mater.* **2**, 206–217 (2013).
12. Lawrence, B. D., Marchant, J. K., Pindrus, M. A., Omenettoa, F. G. & Kaplan, D. L. Silk film biomaterials for cornea tissue engineering. *Biomater.* **30**, 1299–1308 (2009).
13. Marelli, B. *et al.* Compliant electrospun silk fibroin tubes for small vessel bypass grafting. *Acta. Biomaterl.* **6**, 4019–4026 (2010).
14. Lee, M. S., Seo, S. R. & Kim, J. C. A β-cyclodextrin, polyethyleneimine and silk fibroin hydrogel containing centella asiatica extract and hydrocortisone acetate: releasing properties and in vivo efficacy for healing of pressure sores. *Clin. Exp. Dermatol.* **37**, 762–771 (2012).
15. Mandal, B. B., Ghosh, B. & Kundu, S. C. Non-mulberry silk sericin/poly (vinyl alcohol) hydrogel matrices for potential biotechnological applications. *Int. J. Biol. Macromol.* **49**, 125–133 (2011).
16. Bigi, A., Cojazzi, G., Panzavolta, S., Rubini, K. & Roveri, N. Mechanical and thermal properties of gelatin films at different degrees of glutaraldehyde crosslinking. *Biomater.* **22**, 763–768 (2001).
17. Tomihata, K. & Ikada, Y. Cross-linking of gelatin with carbodiimides. *Tissue.Eng.* **2**, 307–313 (1996).
18. Park, S. H. *et al.* Intervertebral disk tissue engineering using biphasic silk composite scaffolds. *Tissue.Eng: Part A.* **18**, 447–458 (2012).
19. Kaplan, D. L., Yucel, T., Lo, T. J. & Leisk, G. G. pH induced silk gels and uses thereof. Patent Application Publication. US2011171239A1.
20. Kundua, J., Poole, L. A., Martens, P. & Kundu, S. C. Silk fibroin/poly(vinyl alcohol) photocrosslinked hydrogels for delivery of macromolecular drugs. *Acta. Biomater.* **8**, 1720–1729 (2012).
21. Wang, X. Q., Kluge, J. A., Leisk, G. G. & Kaplan, D. L. Sonication-induced gelation of silk fibroin for cell encapsulation. *Biomater.* **29**, 1054–1064 (2008).
22. Pritchard, E. M., Valentin, T., Panilaitis, B., Omenetto, F. & Kaplan, D. L. Antibiotic-releasing silk biomaterials for infection prevention and treatment. *Adv. Funct. Mater.* **23**, 854–861 (2012).
23. Seib, F. P., Pritchard, E. M. & Kaplan, D. L. Self-assembling doxorubicin silk hydrogels for the focal treatment of primary breast cancer. *Adv. Funct. Mater.* **23**, 58–65 (2012).
24. Leisk, G. G., Lo, T. J., Yucel, T., Lu, Q. & Kaplan, D. L. Electrogelation for protein adhesives. *Adv. Mater.* **22**, 711–715 (2010).
25. Lu, Q. *et al.* Silk fibroin electrogelation mechanisms. *Acta. Biomater.* **7**, 2394–2400 (2011).
26. Kojic, N. *et al.* Ion electrodiffusion governs silk electrogelation. *Soft.Matter.* **8**, 2897–2905 (2012).
27. Yucel, T., Kojic, N., Leisk, G. G., Lo, T. J. & Kaplan, D. L. Non-equilibrium silk fibroin adhesives. *J. Struct. Biolo.* **170**, 406–412 (2010).

28. Yi, H. *et al*. Biofabrication with chitosan. *Biomacromolecules.* **6**, 2881–2894 (2005).
29. Boccaccini, A., Keim, S., Ma, R., Li, Y. & Zhitomirsky, I. Electrophoretic deposition of biomaterials. *J. R. Soc. Interface.* **7**, 581–613 (2010).
30. Zhang, Z., Jiang, M. K., Cai, X. J., Zhou, Y. & Wang, Y. N. Low temperature electrophoretic deposition of porous chitosan/silk fibroin composite coating for titanium biofunctionalization. *J. Mater. Chem.* **21**, 7705 (2011).
31. Ma, M. M., Zhao, Q. & Tong, Z. Fabrication and voltammetriccharacters of carbon paste electrode modiedusing poly-silk peptide. *J. Fiber. Bioeng. Inform.* **6**, 277–283 (2013).
32. Huang, Y. L., Lu, Q., Li, M. Z., Zhang, B. & Zhu, H. S. Silk fibroin microsphere drug carriers prepared under electric fields. *Sci. China. Press.* **56**, 1013–1018 (2011).
33. Wang, H. Y. & Zhang, Y. Q. Effect of regeneration of liquid silk fibroin on its structure and characterization. *Soft. Matter.* **9**, 138–145 (2013).
34. Zhou, A. H. The effects of different treatment on wool fabric style. *Qual. Tech. Super. Res.* 45–47 (2009).
35. Zhang, Y. Q., Zhou, W. L., Shen, W. D., Chen, Y. H. & Zha, X. M. Synthesis, characterization and immunogenicity of silk fibroin-L-Asparaginase bioconjugates. *J. Biotechnol.* **120**, 315–326 (2005).
36. Ayutsede, J. *et al*. Regeneration of *Bombyx mori* silk by electrospinning. Part 3: Characterizationof electrospun nonwoven mat. *Polymers.* **46**, 1625–1634 (2005).
37. Chen, H., Hu, X. & Cebe, P. Thermal properties and phase transitions in blends of nylon-6 with silk fibroin. *J. Therm. Anal. Calorim.* **93**, 201–206 (2008).
38. Hu, X., Kaplan, D. L. & Cebe, P. Determining beta-sheet crystallinity in fibrous proteins by thermal analysis and infrared spectroscopy. *Macromolecules.* **39**, 6161 (2006).
39. Carey, P. R. Biochemical applications of Raman and resonance Raman spectroscopies. Academic Press, New York. (1982).
40. Monti, P., Freddi, G., Bertoluzza, A., Kasai, N. & Tsukada, M. Raman spectroscopic studies of silk fibroin from *Bombyx mori*. *J. Raman. Spectrosc.* **29**, 297–304 (1998).
41. Rousseau, M. E., Lefèvre, T., Beaulieu, L., Asakura, T. & Pézolet, M. Study of protein conformation and orientation insilkworm and spider silk fibers using Raman microspectroscopy. *Biomacromolecules.* **5**, 2247–2257 (2004).
42. Sirichaisit, J., Brookes, V. L., Young, R. J. & Vollrath, F. Analysis of structure/property relationships in silkworm (*Bombyx mori*) and spider dragline (*Nephila edulis*) silks using Ramanspectroscopy. *Biomacromolecules.* **4**, 387–394 (2003).
43. Hermans, P. H. &Weidinger, A. Quantiative X-ray investigations on the crystallinity ofcellulose fibers. *J. Appl. Phys.* **19**, 491 (1948).
44. Challa, G., Hermans, P. H. & Weidinger, A. On the determination of the crystalline fraction in isotactic polystyrene from X-ray diffraction. *J. Macromol. Chem. Phys.* **56**, 169–178 (1962).
45. Jin,H. J. & Kaplan, D. L. Mechanism of silk processing in insects and spiders. *Nature.* **424**, 1057–1061 (2003).
46. Zhang, Y. Q. *et al*. Formation of silk fibroin nanoparticles in water-miscible organic solvent and theircharacterization. *J. Nanopart. Res.* **9**, 885–900 (2007).
47. Wu, X. L. *et al*. Sodium dodecyl sulfate-induced rapid gelation of silk fibroin. *Acta. Biomater.* **8**, 2185–2192 (2012).
48. Yamada, H., Nakao, H., Takasu, Y. & Tsubouchi, K. Preparation of undegraded native molecular fibroin solution from silkworm cocoons. *Mater. Sci. Eng.* **14**, 41–46 (2001).
49. Zhang, Y. Q. *et al*. Immobilization of L-Asparaginase on the microparticles of the natural silk sericin protein and its characters. *Biomater.* **25**, 3751–3759 (2004).
50. Zhang, Y. Q., Wang, Y. J., Wu, M. H., Wang, H. Y. & Zhu, L. A silk reeling method in strong alkaline electrolyzed water for low temperature. China Patent. 201210082082.X, 2012-3-26.
51. Mandal, B. B., Priya, A. S. & Kundu, S. C. Novel silk sericin/gelatin 3-D scaffolds and 2-Dfilms: Fabrication and characterization for potential tissue engineering applications. *Acta. Biomater.* **5**, 3007–3020 (2009).

Acknowledgments

The authors gratefully acknowledge the earmarked fund (CARS-22-ZJ0504) for China Agriculture Research System (CARS) and a project funded by the Priority Academic Program Development of Jiangsu Higher Education Institutions, P. R. China.

Author contributions

H.Y.W. and Y.Q.Z. designed and performed research. H.Y.W. performed all the experiments and the manuscript text. Y.Q.Z. revised this manuscript. Both authors reviewed the manuscript.

Additional information

Competing financial interests: The authors declare no competing financial interests.

How to cite this article: Wang, H.-Y. & Zhang, Y.-Q. Processing and characterisation of a novel electropolymerized silk fibroin hydrogel membrane. *Sci. Rep.* **4**, 6182; DOI:10.1038/srep06182 (2014).